Article

Collision Strengths of Astrophysical Interest for Multiply Charged Ions

Stephan Fritzsche [1,2,3,*], Li-Guang Jiao [1,2,4], Yuan-Cheng Wang [1,2,5] and Jozef E. Sienkiewicz [6]

1   Helmholtz-Institut Jena, Fröbelstieg 3, 07743 Jena, Germany
2   GSI Helmholtzzentrum für Schwerionenforschung, 64291 Darmstadt, Germany
3   Theoretisch-Physikalisches Institut, Friedrich-Schiller-Universität Jena, 07743 Jena, Germany
4   College of Physics, Jilin University, Changchun 130012, China
5   College of Physical Science and Technology, Shenyang Normal University, Shenyang 110034, China
6   Faculty of Applied Physics and Mathematics and Advanced Materials Center,
    Gdańsk University of Technology, 80-233 Gdańsk, Poland
*   Correspondence: s.fritzsche@gsi.de

Abstract: The electron impact excitation and ionization processes are crucial for modeling the spectra of different astrophysical objects, from atmospheres of late-type stars to remnants of supernovae and up to the light emission from neutron star mergers, to name just a few. Despite their significance, however, little is known quantitatively about these processes for low- and medium-impact energies of, say, $E_{kin} \lesssim 5000$ eV of the free incident electron. To further explore the role of impact excitation, we here expanded JAC, the Jena Atomic Calculator, to the computation of distorted wave collision strengths for fine-structure-resolved, as well as configuration-averaged transitions. While we excluded the formation of dielectronic resonances, these tools can be readily applied for ions with a complex shell structure and by including the major relativistic contributions to these strengths. Detailed computations of the collision strengths are shown and explained for the impact excitation of lithium- and chlorine-like ions. When compared with other, well-correlated methods, good agreement was found, and hence, these tools will support studies of effective collision strengths for a wide range of electron impact energies, levels, and ionic charge states.

Keywords: atomic structure; (effective) collision strength; distorted wave; electron impact excitation; fine-structure-resolved; Jena Atomic Calculator; multiply charged ion; non-resonant strength; relativistic

1. Introduction

The electron impact excitation (EIE) of atoms and ions generally refers to an inelastic (scattering) process, in which a free electron interacts with the bound state density and leaves the atom in an excited state. Such scattering processes are known to occur frequently in all kinds of plasma and electron beam devices. In plasma diagnostics, for example, accurate EIE cross-sections are needed for determining the temperature, density, or level population of excited states [1,2]. In non-local thermodynamic equilibrium (non-LTE) plasma, moreover, the impact excitation cross-sections and collision strengths are required to deduce the spectral line intensities of light curves as observed, for instance, from rapidly expanding astrophysical objects [3,4], sometimes known as the non-LTE line formation problem. The collision strengths are important ingredients also for most radiative transfer simulations that help explore the evolution of stellar atmospheres [5], magnetospheres [6], or other astrophysical objects. Figure 1 summarizes several applications of the collision strengths and EIE cross-sections in astro and plasma physics.
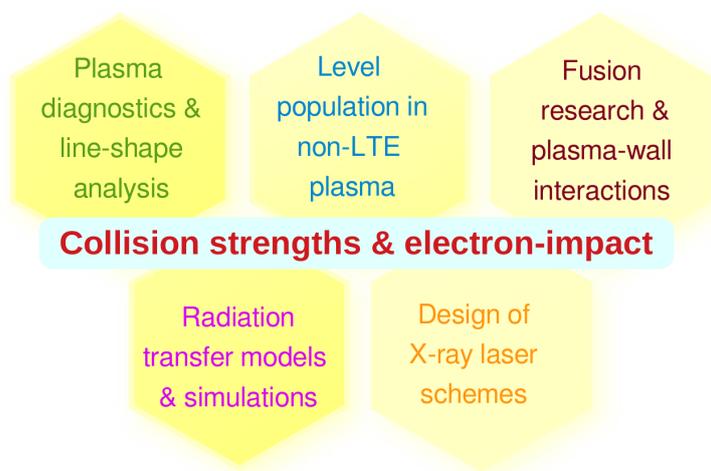
Figure 1. Application of collision strengths in astro and plasma physics, as well as for the development of new light sources.

For multiply charged ions, the necessary collision strengths have been calculated, more often than not, in the plane wave Born approximation [7,8], in which the excitation into different (excited) states is assumed to be independent of each other [9]. Apart from the first-Born approximation, the Coulomb or distorted wave (DW) Born approximation accounts for the modification of the—incoming and scattered—electron waves owing to the Coulomb *or* some realistic many-electron potential of the (excited) atoms or ions [10,11]. When based on Dirac's equation, the DW Born approximation also includes the relativistic level splitting and the contraction of the electron density in medium and heavy elements, while it still neglects the resonant capture of free electrons, which is known to become relevant at low impact energies.

Fine-structure-resolved collision strengths $\Omega(\varepsilon; i \rightarrow f)$ for transitions $i \rightarrow f$ between bound state levels by free electrons with impact energy ε are indeed the main ingredient for providing impact excitation cross-sections and plasma rate coefficients of various kinds. Following the earlier work by Zhang and coworkers [12–14], we here expanded JAC, the Jena Atomic Calculator [15], towards readily accessible collision strength computations for multiply and highly charged ions of astrophysical interest. Although a number of similar codes *do* exist in the literature [12,16,17], they are usually not publicly available, nor can the generated data be compared so easily with each other and with the data from the literature. Difficulties in dealing with and comparing collision strengths from different sources often arise not only from the precise definition of these strengths or the use of different input parameters, but also from a good number of (short-hand) notations that can hardly be resolved in full detail. Until the present, therefore, little insight exists into the accuracy, as well as the energy and shell structure dependence of the collision strength for multiply charged ions. By expanding the JAC toolbox, we provide direct access to these dependencies, along with a simple setting of the levels involved, the interelectronic interaction, and the units in compiling the collision strength or any related property for ions of astrophysical interest.

In the next section, we first recall the basic expressions for calculating the (non-resonant) collision strengths and EIE cross-sections. Apart from the transition amplitude in the DW approximation, we here remind the reader also of challenges in dealing with the free electron continua, as well as of the practical needs for generating useful strengths for astrophysics. These needs are then mirrored both by the data structures for handling symmetry-adapted collision strengths, as well as the (modular) implementation within the JAC toolbox. For the sake of illustration in using these tools, Section 3 reports and compares the level- and energy-dependent collision strengths for selected lithium- and chlorine-like ions. Finally, a short summary and a few conclusions are given in Section 4.

2. Theory and Implementation

2.1. Electron Impact Excitation versus Dielectronic Capture with Subsequent Re-Autoionization

All electron impact processes of atoms and ions arise from and are dominated by the interaction between the free (incoming) electron with the bound state density. This interaction not only gives rise to the inelastic (and non-resonant) scattering of the electron by the atom, but also determines the strength of the resonant capture to form ions of the next lower charge state, which then contribute to the impact excitation by their subsequent re-autoionization. These resonant contributions to the collision strength at well-defined energies of the doubly excited ion can be typically modeled as a two-step process, in which the first step is equivalent to the dielectronic capture into an excited state of the atom or ion [18,19]. In such a two-step model, the total EIE collision strength for a fine-structure transition $i \to f$ or, equivalently, $\alpha_i \mathbb{J}_i \to \alpha_f \mathbb{J}_f$ is given by

$$\Omega^{(\text{EIE:total})}(\varepsilon; i \to f) = \Omega^{(\text{EIE})}(\varepsilon; i \to f) + \sum_d \Omega^{(\text{DC})}(\varepsilon; i \to d) \, B(d \to f)$$

where ε is the (asymptotic) kinetic energy of the incident electron, $\Omega^{(\text{DC})}(\varepsilon; i \to d)$ the electron capture strength into the resonance d with total energy $E_d = E_i + \varepsilon$, and $B(d \to f)$ the branching ratio for the re-autoionization of the doubly excited $((N+1)$-electron$)$ ion into the final level f. This branching ratio accounts for the competition that the resonance d may decay also due to other radiative and non-radiative channels. In a more detailed notation, $\alpha_i \mathbb{J}_i \to \alpha_f \mathbb{J}_f$ provides here with $\mathbb{J} \equiv J^P$ a useful short-hand notation for both the total angular momentum J and parity P of the many-electron levels, while $\alpha_{i,f}$ refer to all further quantum numbers that are needed to classify the atomic levels uniquely [20,21].

In this contribution, we focused on the (non-resonant) EIE collision strength $\Omega^{(\text{EIE})}(\varepsilon; i \to f)$. The total strength $\Omega^{(\text{EIE:total})}(\varepsilon; i \to f)$ can be determined also directly from various close-coupling approaches, if a sufficiently large number of bound $(N+1)$-electron resonances, embedded into the N-electron continuum, are taken into account. In practice, the resonant contributions to the total EIE collision strength are usually considered small or at least less relevant, $\Omega^{(\text{EIE:total})}(\varepsilon; i \to f) \approx \Omega^{(\text{EIE})}(\varepsilon; i \to f)$, if the energy-dependent EIE collision strengths are requested for a wide range of incident energies ε. We leave it to the readers to accept this approximation when the collision strengths are to be applied to multiply and highly charged ions.

2.2. Collision Strengths and Electron Impact Excitation Cross-Sections

The term *collision strength* was first suggested by Seaton [22] and naturally arises from describing the inelastic scattering of atoms and ions perturbatively. This collision strength is closely related also to the EIE cross-section by

$$\sigma^{(\text{EIE})}(\varepsilon; i \to f) = \frac{4\pi a_o^2}{k_i^2 \, (2J_i + 1)} \, \Omega^{(\text{EIE})}(\varepsilon; i \to f), \tag{1}$$

if the wave function of the free electrons (see below) is properly normalized per unit energy: $\langle \psi(\varepsilon) | \psi(\varepsilon') \rangle = \delta(\varepsilon - \varepsilon')$. In this formula, $k_i = k_i(\varepsilon)$ is the wave number of the free incident electron, and the factor $(2J_i + 1)$ in the cross-section Equation (1), i.e., the statistical weight of the initial level i in the notation above, ensures the simple symmetry relation $\Omega^{(\text{EIE})}(\varepsilon; i \to f) = \Omega^{(\text{EIE})}(\varepsilon; f \to i)$, as expected from the interaction amplitude in Equation (2).

Here, we shall not discuss the so-called transition matrix T nor (any approximation to) the reactance matrix R from formal time-independent scattering theory [23,24]. If the

incident and scattered electrons are described in terms of the partial waves $|\varepsilon\,\kappa_i\rangle$ and $\left|\varepsilon_f\,\kappa_f\right\rangle$, the collision strength in (relativistic) atomic structure theory is simply given by [12]

$$\Omega^{(\mathrm{EIE})}(\varepsilon; i \to f) \quad = \quad 2 \sum_{\kappa_i,\kappa_f} \sum_{\mathbb{J}_t} [J_t] \left| \left\langle (\mathbb{J}_f, \epsilon_f\,\kappa_f)\mathbb{J}_t \middle\| \mathbb{V}^{(\mathrm{e--e})} \middle\| (\mathbb{J}_i, \epsilon\,\kappa_i)\mathbb{J}_t \right\rangle \right|^2, \qquad (2)$$

i.e., as the sum of reduced matrix elements of the electron–electron (e–e) interaction operator $\mathbb{V}^{(\mathrm{e--e})}$, but taken with regard to the scattering states on the left- and right-hand side of Equation (2), each with a single free electron in the continuum. In the DW approximation, the initial and final energies of the scattered electron are related to each other by the total energies E_i, E_f of the atomic bound states due to energy conservation: $E_{fi} = E_f - E_i = \varepsilon - \varepsilon_f$. In this expression, moreover, the e–e interaction amplitudes for the zero-rank operator $\mathbb{V}^{(\mathrm{e--e})}$ are standard to atomic structure theory and occur quite similarly in the setup of the Hamiltonian and autoionization matrices [25–27], whereas $[J_t] = 2J_t + 1$ denotes the statistical weight of the scattering states. However, special care has to be taken that a free electron now occurs on both sides of the matrix elements [28,29]. We also note that Equation (2) for the collision strength generally gives rise to ununitarized excitation cross-sections because of the approximations, which are made to the original transition matrix T. For multiply and highly charged ions, this is normally considered as a reliable approximation.

While the collision strength $\Omega^{(\mathrm{EIE})}(\varepsilon; i \to f)$ is formally defined to be of order one for electric dipole transitions, the individual strengths typically exhibit (very) large variations owing to the electronic structure of the (target) ions, as well as the oscillating behavior of the free electron wave as its kinetic energy varies [17]. Indeed, these variations are central to the computations below and do certainly *not* suggest approximating $\Omega^{(\mathrm{EIE})}(\varepsilon; i \to f) \equiv \mathrm{const.}$, as is sometimes performed in radiative transfer simulations.

The collision strength (2) in the DW approximation has been found useful also for providing EIE cross-sections for fusion research or the design of X-ray lasers [30]. For these applications, (the account of) the relativistic structure of the bound electrons is usually more important than improvements of the scattering theory beyond distorted waves. In our implementation below, we made use of the Dirac–Hartree–Slater method to generate the wave functions of the bound ions, as well as the configuration-averaged (central) potential for generating the partial waves of the free electron. Not much needs to be said about the computation of approximate atomic state functions (ASFs), as well as the basic theory, which can be found in various texts, cf. [25,31]. In addition to the usual (instantaneous) Coulomb repulsion between the incident and the target electrons, the pairwise interaction between the electrons is sometimes better described by the sum of this Coulomb term and the (so-called) *transverse* Breit interaction b_{ij}:

$$\mathbb{V}^{(\mathrm{e--e})} \quad = \quad \mathbb{V}^{(\mathrm{Coulomb})} + \mathbb{V}^{(\mathrm{Breit})} \quad = \quad \sum_{i<j} \left(\frac{1}{r_{ij}} + b_{ij} \right) \qquad (3)$$

in order to account for the *relativistic* motion of the electrons. In practice, the Breit interaction is typically taken in its frequency-independent form as appropriate for most computations. For medium and heavy elements, moreover, the decision about the particular form of the e–e interaction operator $\mathbb{V}^{(\mathrm{e--e})}$ is usually based on physical arguments, such as the nuclear charge, the charge state of the ion, or the shell structure of interest [32,33]. Furthermore, a common central potential for all partial waves of fixed energy ε (or ε_f) accelerates the computation of the e–e interaction matrix elements by an order of magnitude and is well in line with the DW ansatz.

In the JAC toolbox, all ASF and e–e interaction amplitudes are expressed and evaluated in terms of symmetry-adapted configuration state functions (CSFs). These amplitudes are the central building blocks of JAC and can be readily obtained for further data processing. To compute the collision strengths (2), the standard decomposition of the e–e interac-

tion matrix elements in terms of angular coefficients and effective interaction strengths $X_L(abcd) = X_L^{(\text{Coulomb})}(abcd) + X_L^{(\text{Breit})}(abcd)$ is utilized and where the Breit interaction can be added, if this appears appropriate for a given ion and excitation process. Since the Coulomb and Breit interaction operators are both scalar and contribute *additively* to the total e–e interaction, the same (pure) angular coefficients occur in the evaluation of amplitudes in Equation (2), although different angular and parity selection rules apply for the various interaction strengths [34,35]. When compared with a purely nonrelativistic (Coulomb) treatment, the number of radial matrix elements increases, however, roughly by a factor of 10 to 30 within the full relativistic (atomic) theory.

In a single-configuration approach to the collision strength, the computation of the e–e interaction amplitudes in Equation (2) can be simplified by recoupling the partial waves in such a way that the contributions from the bound state electrons can be factored out [36]. This treatment is based on configuration-averaged energies and assumes that all radial integrals only weakly depend on the energies of the scattered electron. When compared with the standard techniques for calculating collision strengths, such a configuration-averaged procedure drastically reduces the number of radial integrals that need to be evaluated. A similar reduction can be achieved by re-using and compiling the angular coefficients before the effective interaction strengths are calculated.

Several alternatives have been developed and applied for computing EIE cross-sections for atoms and ions, including the convergent close-coupling [37], R-matrix close-coupling [38], or time-dependent close-coupling scheme [39]. These advanced methods enable one to partly incorporate resonances and the coupling between different excitation channels [40]. When compared to the DW approach (2), however, these inherently correlated methods are (much) more elaborate and typically require large-scale (or even parallel) computations. They are normally restricted also to ions with a simple shell structure. In practice, moreover, the position and strength of the resonances often appear quite sensitive to the details of the computations and can be rarely compared explicitly to measurements.

2.3. Generation and Use of Collision Strengths for Astrophysical Modeling

While the (decomposition of the) e–e interaction matrix elements have been optimized for calculating accurate bound state energies or (auto)ionization rates, electron impact processes typical impose a larger challenge. Computational demands arise not only from the free electron in both the incoming and outgoing scattering states, but also from the large number of channels that need to be taken into account. Unlike photoionization cross-sections, which typically require just a few continuum orbitals due to well-established selection rules, EIE cross-sections often imply a good number of continuum orbitals in any relativistic (and nonrelativistic) formulation, because they obey for the partial waves much less strict selection rules. For many applications in astrophysics and elsewhere, in addition, these cross-sections need to be known for different impact energies and for a number of excited levels $\alpha_f \mathbb{J}_f$. In several previous implementations [41–43], it has, therefore, been found useful to calculate the collision strengths at a given set of incident (or outgoing) energies and independent of the selected transitions, since these collision strengths often vary slowly with energy. Moreover, several interpolation schemes have been utilized to keep the computations feasible, although this interpolation of the strengths with regard to the free electron energies is also a source of inaccuracy and needs to be performed with care. A further simplification is sometimes made, if all the partial waves are generated with the same averaged potential of the (target) ion, which reduces the compute time by roughly an order of magnitude.

The fine-structure-resolved collision strengths (2) are the main key to understanding the excitation of atoms and ions by electron impact. Often, however, ions exhibit a rather complex shell structure already in their ground configuration. For heavy and ionized atoms with open *d*- and *f*-shells, the fine structure of single initial- and final-state configurations may then lead to hundreds of (fine-structure) transitions with tiny splittings in energy [44]. For such ions, the configuration-averaged collision strength and cross-sections are, there-

fore, required for most applications and will make simple and robust tools desirable for estimating (effective) collision strengths and rate coefficients of different sorts.

In a (Maxwellian) plasma, for example, the *effective* collision strength for an atomic transition $i \rightarrow f$ is given by

$$\Omega^{(\mathrm{eff})}(T_e; i \rightarrow f) \quad = \quad \frac{1}{k T_e} \int_{\Delta E}^{\infty} d\varepsilon \, \Omega^{(\mathrm{EIE:total})}(\varepsilon; i \rightarrow f) \, \exp\left(\frac{\varepsilon}{k T_e}\right),$$

where T_e is the electron temperature and $\Delta E = E_f - E_i = \varepsilon - \varepsilon_f$ the excitation energy of the transition, where a Maxwellian distribution is used to average over the (total) collision strength. Similarly, the EIE plasma rate coefficient describes the excitation rate for the transition $i \rightarrow f$ of a single ion in the level $\alpha_i \mathbb{J}_i$ per unit volume. This rate coefficient is obtained, as usual, from the convolution of the cross-section $\sigma(\varepsilon; i \rightarrow f)$ with a Maxwellian electron distribution as

$$\alpha^{(\mathrm{EIE})}(T_e; i \rightarrow f) \quad = \quad \frac{4}{(k_B T_e)^{3/2}\sqrt{2\pi m}} \int_{\Delta E}^{\infty} d\varepsilon \, \varepsilon \, \sigma^{(\mathrm{EIE})}(\varepsilon; i \rightarrow f) \, \exp\left(\frac{\varepsilon}{k_B T_e}\right) \qquad \left[\frac{\mathrm{cm}^3}{\mathrm{s}}\right].$$

Moreover, by averaging over several final states, the plasma rate coefficient simply becomes

$$\alpha^{(\mathrm{EIE})}(T_e; i \rightarrow \{f\}) \quad = \quad \sum_{\{f\}} \alpha^{(\mathrm{EIE})}(T_e; i \rightarrow f).$$

Until the present, there is only limited agreement in the literature on how these effective strengths are to be defined and employed in applications. From the various requests above, however, we easily infer the need for having alternative implementations of these rate coefficients in order to extract useful data for astrophysically relevant ions.

2.4. Data Structures for Symmetry-Adapted Collision Strengths

Well-designed data structures are crucial for any modern implementation of electronic structure theory for atoms, ions, and many places elsewhere. These structures should define the central objects in order to facilitate the transfer of data within the program and its communication with the user. For any correlated computation of collision strengths, these data structures must provide also a simple access and distinction of all ingredients in Equation (2), including the atomic bound states, partial waves of the incoming and outgoing electrons, or the e–e interaction operator in the transition matrix elements, to recall just a few. In practice, these data structures form the (language) elements in order to describe and control the desired computations, with a notion that is readily understandable to most atomic physicist (and potential users of the code).

To obey these needs, we chose Julia as a new and recently established language for scientific computing [45]. This (compute) language helps to clearly articulate data in a suitable form for physics. It is also built by default on dynamic arrays, whose size can grow by pushing further data to it, based on some sophisticated algorithm. Julia also works like a functional language, where functions operate on data types and data structures. When compared with other programming languages, Julia's type system in particular is known as one of its strongest features, in which abstract data types may help establish a hierarchy of relationships between data and actions and, hence, model *behavior*. In Julia, indeed, all types are said to be first-class and are utilized to select the code dynamically by means of (so-called) multiple dispatch. For electronic structure calculations, a few important (examples of such) data types are an `orbital` to represent the quantum numbers and radial components of the (one-electron) orbital functions, an atomic `basis` to specify a set of many-electron CSFs, or a `level` for the full representation of a single ASF: $E, |\alpha \mathbb{J}M\rangle$, as occurs in the middle panel of Figure 2. In total, JAC is built on about $\sim$250 of these data structures, though most of them remain hidden to the user.

```
struct ImpactExcitation.Channel
    ... defines a type for an electron-impact excitation channel that characterizes the incoming and
        outgoing (scattering) states of many-electron atoms with a single free electron each.

  + initialKappa      ::Int64            ... Partial-wave of the incoming free electron.
  + finalKappa        ::Int64            ... Partial-wave of the outgoing free electron.
  + symmetry          ::LevelSymmetry    ... Total angular momentum & parity of both scattering states.
  + initialPhase      ::Float64          ... Phase of the incoming partial wave.
  + finalPhase        ::Float64          ... Phase of the outgoing partial wave.
  + amplitude         ::Complex{Float64} .. Collision amplitude associated with the given channel.
```

```
struct ImpactExcitation.Line
    ... defines a type for a electron-impact excitation line that is based on a set of excitation
        channels and their associated amplitudes.

  + initialLevel            ::Level        ... Initial- (bound-state) level.
  + finalLevel              ::Level        ... Final- (bound-state) level.
  + initialElectronEnergy   ::Float64      ... Energy of the incoming (initial-state) free-electron.
  + finalElectronEnergy     ::Float64      ... Energy of the outgoing (final-state) free-electron.
  + crossSection            ::Float64      ... Total cross section of this line.
  + collisionStrength       ::Float64      ... Total collision strength of this line.
  + channels                ::Array{ImpactExcitation.Channel,1}
                                           ... List of associated ImpactExcitation channels.
```

```
struct ImpactExcitation.Settings <: AbstractProcessSettings
    ... defines a type for the control parameters of computing electron-impact excitation lines.

  + electronEnergies    ::Array{Float64,1} ... List of impact-energies of the incoming electron
                                               (in user-defined units).
  + printBefore         ::Bool             ... True, if all energies and lines are printed before
                                               their evaluation.
  + lineSelection       ::LineSelection    ... Specifies the selected excitation lines, if any.
  + energyShift         ::Float64          ... An overall energy shift for all transitions i -> f.
  + maxKappa            ::Int64
        ... Maximum kappa value of partial waves to be included into the computations.
  + operator            ::AbstractEeInteraction
        ... Interaction operator that is to be used for evaluating the e-e interaction amplitudes;
            allowed values are: CoulombInteraction(), BreitInteraction(), CoulombBreit().
```

Figure 2. Important data structures from the `ImpactExcitation` module of JAC for the computation of EIE cross-sections and collision strengths.

A few such data structures are particularly useful to facilitate the computation of collision strengths and EIE cross-sections in the implementation below. These data structures refer to a single excitation line $i \rightarrow f$ of the bound ion, as well as to the partial waves $|\varepsilon\,\kappa_i\rangle$ and $\left|\varepsilon_f\,\kappa_f\right\rangle$ for constructing the scattering states of well-defined symmetry $\mathbb{J}_t$. For each excitation line (transition), obviously, a rather large number of partial waves occur, all with energies ε for the incoming electron and ε_f for the scattered electron. As for the photoionization or autoionization of ions, it appears useful to distinguish between `ImpactExcitation.Channels` and `ImpactExcitation.Lines` in order to keep all relevant information together. The upper and middle panels of Figure 2 display the definition of the associated data structures as specified in the `ImpactExcitation` module. A channel hereby comprises the total angular momentum and parity (`symmetry`), as well as the quantum numbers (κ_i, κ_f) of the partial waves. All these channels belong to the same EIE line with electron energies ε and ε_f and come along with a full specification of the initial and final levels. Eventually, `ImpactExcitation.Line` contains `crossSection` and `collisionStrength` in order to facilitate the compilation of data at the final stage of the computation. The distinction between channels and lines also enables one to benefit from the decomposition of the amplitude into angular coefficients and effective interaction strengths, similar to the

work of Bar-Shalom and coworkers [36]. In the present implementation, this is achieved by re-applying certain angular coefficients (and parts of the interaction strength) to obtain the amplitudes of subsequent channels. This distinction may open also a simple avenue to compute in future the amplitudes in parallel in order to cope with the large number of partial waves on each side of Equation (2).

The lower panel of Figure 2 displays `ImpactExcitation.Settings` and how these settings can be utilized to control the computations below. These settings are further discussed in Section 3.1 and are shown in Table 1, along with a few selected data structures that are relevant for the computation of collision strengths. Here, all these data structures are explained only briefly, while further details can be obtained from the manual to the JAC toolbox [21] or by using Julia's help facilities[1]. These structures are helpful for the reader (and user of JAC) to better understand and possibly control the computations of interest.

Table 1. Selected data structures of the JAC toolbox as needed for the computation of electron impact excitation cross-sections and collision strengths.

Struct and Brief Explanation.
`AbstractEeInteraction`: defines an abstract, as well as a number of singleton types for specifying the e–e interaction; valid subtypes are `CoulombInteraction()`, `BreitInteraction()`, and `CoulombBreit()`.
`AbstractProcessSettings`: defines an abstract type to distinguish between different settings of atomic processes, such as `AutoIonization.Settings`, `PhotoIonization.Settings`, `PhotoRecombination. Settings`, ..., and several others.
`Level`: a data type for an atomic level $\alpha \mathbb{J}$ in terms of its quantum numbers, energy, and a representation with regard to a given relativistic CSF basis.
`LevelSymmetry`: specifies the overall $\mathbb{J} \equiv J^P$ symmetry of a level.
`LineSelection`: helps specify a list of level pairs by means of their (level) indices or level symmetries.
`ImpactExcitation.Channel`: characterizes the incoming and outgoing (scattering) states of many-electron atoms or ions with a single free electron; cf. the upper panel of Figure 2.
`ImpactExcitation.Line`: specifies an EIE line, based on the definition of the initial and final levels, the impact excitation channels above, and the e–e interaction amplitudes; cf. the middle panel of Figure 2.
`ImpactExcitation.Settings`: specifies all control parameters for the computation of the EIE lines.

2.5. Computation of Collision Strengths with the Jena Atomic Calculator

In general, the calculated collision strengths cannot be more reliable than the underlying representation of the initial and final bound levels (i, f), nor the partial waves as obtained within the potential of the ion. To generate these representations, we made use of and expanded JAC, the Jena Atomic Calculator, to readily access all ingredients of the e–e interaction amplitudes in Equation (2) and, hence, the required strengths and cross-sections. Indeed, this toolbox supports atomic (structure) calculations of different kinds and complexities, and it can be easily applied also to model different atomic excitation and decay processes within the same computational framework. With the design and implementation of JAC, we aimed to develop a "descriptive language" that is (i) user-friendly, (ii) emphasizes the underlying atomic physics, and (iii) avoids most technical jargon, as is common for many established atomic codes from the literature. All these goals are relevant in order to ensure a good (self-)consistency of the data generated for different atomic properties and processes. The JAC toolbox has been described elsewhere [15,21] and can be downloaded from the web [21], including the present extension.

During the past few years, JAC has been (enlarged and) applied to the computation of level structures and decay rates of open shell atoms, the prediction of DR resonance spectra and plasma rate coefficients [19], the photorecombination for multiply charged ions [46], as well as for simulating atomic cascades and photon emission spectra [47]. It has been applied especially to model a number of decay cascades as relevant for astrophysical

observations [48–50]. Since JAC is based on Dirac's relativistic equation, it is well suited also to computing atomic data for multiply charged, as well as medium and heavy ions.

In this work, we added the computation of collision strengths to JAC. Apart from the generation of all partial waves for the—incoming and outgoing—free electrons, this implies the proper coupling of electrons in the construction of the scattering states, as well as the evaluation of the e–e interaction amplitudes in Equation (2). In some more detail, the distorted waves were hereby generated in a configuration-averaged potential of the ion. In practice, the representation of the bound state levels and the continuum orbitals, along with all the associated approximations in dealing with the atomic levels and scattering states, make the main differences between the implementations that are available from the literature. This includes also the particular choice of the e–e interaction operator $\mathbb{V}^{(e--e)} = \mathbb{V}^{(Coulomb)} + \mathbb{V}^{(Breit)} \approx \mathbb{V}^{(Coulomb)}$, which, in principle, enables one to incorporate relativistic corrections due to the Breit interaction into the collision strengths and which has attracted previous attention for multiply and highly charged ions [51]. A further distinction of the JAC toolbox refers to the quite consequent use of the many-electron interaction amplitudes, quite in contrast to most other atomic structure codes, which facilitates the implementation of new features to the code.

As for most other processes, JAC's `Atomic.Computation` now helps access also the EIE cross-sections and collision strengths. These `Atomic.Computations` are always based on explicitly specified electron configurations and have been designed to automatically calculate the underlying level energies and representations of all ASFs of interest. These `computations`, therefore, enable one to obtain the (correlated) collision strengths between individual fine-structure levels or for a set of such levels as a whole and as derived from the initial and final configurations. Separate self-consistent field calculations were carried out to generate the fine structure in the initial and final state of the ion. These computations can be furthermore controlled by *settings* that are specific to some given property or process, which are shown in the lower panel of Figure 2 for the EIE process. Apart from the (list of) energies of the incident electron, these settings help the user select individual excitations (lines) of the target ion or determine a maximum κ_{max} in the partial-wave expansion of the free electrons. They also support some printout prior to the computation, a constant energy shift of all excitation energies, as well as the choice of the e–e interaction mentioned before. Whereas default values are provided for all these parameters, they can easily be overwritten by the user on demand. Further control parameters might be added in the future to enhance the efficiency or the scope of the computations. Aside from the `Atomic.Computation` above, several procedures from the `ImpactExcitation` module can be called also interactively by the user and will allow implementing further extensions of the JAC toolbox as summarized in Section 2.3 above. While the computational efficiency of the present implementation is comparable to other existing codes [12,16], the use of default parameters and their simple re-definition by the user provides a strong benefit and will facilitate further extensions and studies with JAC.

3. Level- and Energy-Dependent Collision Strengths for Multiply and Highly Charged Ions

Collision strengths have been calculated (and tabulated) for a number of light, medium, and heavy ions, cf. [52,53] and—more recently—also for fine-structure-resolved, low-lying excitations of ions with a complex shell structure, such as germanium-like [54] or even Co^{2+} ions with an open $3d$ shell [55]. Despite the need for such data for radiation transfer or non-LTE simulations, the good number of notations for specifying the energies, shell coupling, and quantum numbers of the ionic levels involved, as well as different averaging procedures have surely hampered the use and comparison of collision strengths in the literature. Besides missing information about the initial and final bound state levels, limitations often arise from the selective choice of elements, charge states, the range of incident energies, or units (as typical input parameters). By using JAC, we wish to show

how readily such an energy-dependent collision strength can be generated with a rather simple and transparent setting of the various parameters.

3.1. Collision Strengths for Lithium-like Neon and Iron

Lithium-like ions are perhaps the simplest many-electron systems for which collision strengths have been calculated in the past, which are little affected by resonances at moderate collision energies. For these ions, EIE cross-sections and collision strengths were calculated in a distorted wave approximation for $2s - np$ $(n = 2, 3)$ transitions in [13,17,56] and at several places elsewhere. Impact excitation cross-sections for these ions have been measured also in electron beam ion trap (EBIT) devices, though typically not on an absolute scale. For multiply and highly charged ions, a fully relativistic approach is hereby needed for the accurate calculation of cross-sections and collision strengths.

For the $2s - 2p$ EIE of lithium-like Ne^{7+} ions, for example, the (non-resonant) collision strengths can be calculated by means of the JAC toolbox by just following Figure 3. This figure displays the input for `Atomic.Computation` with JAC. Apart from selecting the units and the method for obtaining the continuum orbitals, a name (string), as well as the radial grid, appropriate for continuum processes, we only need to provide the nuclear charge ($Z = 10$) and the configurations for the initial and final levels of the bound ion. Further configurations could be included in these lists to improve the "correlated" representation of the bound levels, though for the price of rapidly increasing computational costs. The computations then include the configuration mixing among all those levels that can be formed from these configurations. In practice, however, mainly the number of configurations and channels, i.e., the maximum $\kappa_{\max}$ in the partial-wave expansion, decides about the effort in the computation of EIE cross-sections and collision strengths. A value of $\kappa_{\max}$ between 12 and 20 has been found sufficient for impact energies $\varepsilon \lesssim 5000$ eV to obtain reasonably stable results. Of course, all these calls in Figure 3 can be made also linewise to immediately see and check the consistency of the given specification. Here, we do not print the output explicitly, but display the obtained collision strengths in the left panel of Figure 4. Some further work is likely needed to accelerate, and perhaps parallelize, these computations for other shell structures, while the given input will remain quite similar or even the same. For collision strengths, the full convergence of the data with regard to the expansions of the initial and final bound states can hardly be monitored because of the unfavorable increase of the computational costs. Apart from core–valence and valence–valence correlations, moreover, the shake-up of valence electrons may contribute to the overall EIE cross-section, but is usually not treated explicitly within any DW approximation.

```
# Collision strengths for lithium-like Ne^7+ ions; 2s - 2p_1/2,3/2
setDefaults("method: continuum, Galerkin")
setDefaults("unit: cross section", "barn");     setDefaults("unit: energy", "eV")

grid = Radial.Grid(Radial.Grid(false), rnt = 4.0e-6, h = 5.0e-2, hp = 1.0e-2, rbox = 10.0)
comp = Atomic.Computation(Atomic.Computation(), name="2s-2p impact excitation of lithium-like Ne.",
                    nuclearModel    = Nuclear.Model(10.), grid=grid,
                    initialConfigs  = [Configuration("1s^2 2s")],
                    finalConfigs    = [Configuration("1s^2 2p")],
                    processSettings = ImpactExcitation.Settings([100., 400., 700.],
                        true, true, true, LineSelection(true, indexPairs=[(1,1), (1,2)]),
                        0., 16, CoulombInteraction()) )
perform(comp)
```

Figure 3. Input to the JAC toolbox for the `Atomic.Computation` of EIE cross-sections and the collision strength for the $2s - 2p$ transitions of lithium-like neon and for impact energies $\varepsilon = 100$, 400 and 700 eV.
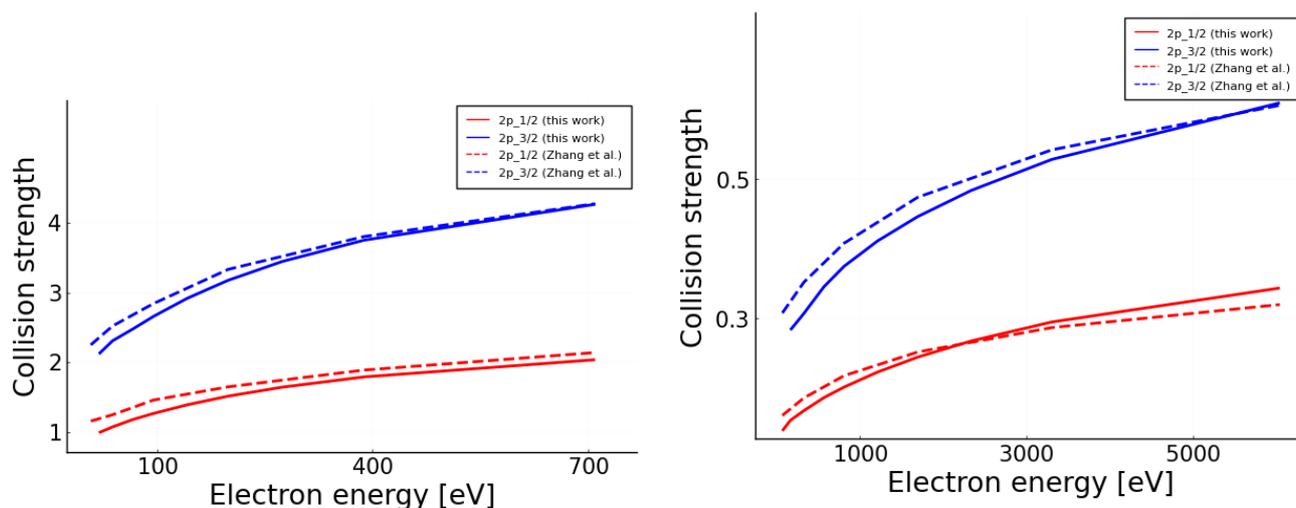
Figure 4. Collision strength $\Omega(\varepsilon; i \rightarrow f)$ as a function of the initial electron energy ε (eV) for lithium-like Ne^{7+} (**left panel**) and Fe^{23+} ions (**right panel**). Left: Results from this work are shown for the $2s - 2p_{1/2}$ (red solid lines) and for the $2s - 2p_{3/2}$ excitation (blue solid lines) and are compared with the computations by Zhang et al. ([14]; dashed lines).

Figure 4 displays the collision strength $\Omega(\varepsilon; i \rightarrow f)$ as a function of the initial electron energy ε for lithium-like Ne^{7+} (left panel) and Fe^{23+} ions (right panel). Results from this work are shown for the $2s - 2p_{1/2}$ (red solid lines) and for the $2s - 2p_{3/2}$ excitations (blue solid lines) and were compared with similar computations by Zhang and coworkers ([14]; dashed lines). As seen from these figures, the collision strength increased monotonically with the impact energy and in good agreement with previous computations. For low impact energies, small deviations occurred due to the different representation of the atomic bound states. For the $2s - 2p_{3/2}$ excitation, the collision strengths were roughly twice those for $2s - 2p_{1/2}$ owing to the statistical weight of the $2p_{3/2}$ shell. However, this difference became smaller at high impact energy and for ions with a large charge Z due to relativistic effects. Similar computations as in Figure 3 were performed also to produce the other figures, including the excitation of inner-shell electrons.

Figure 5 displays analogue collision strengths for lithium-like iron and at impact energies suitable for the $1s - 2p$ and $1s - 3d$ inner-shell excitation. Computations are shown on the left panel for the $1s^2 2s\ ^2S_{1/2} - 1s2s2p\ ^4P_J$ levels with $J = 1/2$ (red line), $J = 3/2$ (blue line), and $J = 5/2$ (green line) and on the right panel of Figure 5 for the $1s^2 2s\ ^2S_{1/2} - 1s2s3d\ ^4P_J$ levels with $J = 1/2, 3/2, 5/2$, and $7/2$, respectively. For all these fine-structure-resolved transitions, the collision strengths rapidly decrease with increasing energy of the incident electron. At rather similar impact energies, moreover, the non-electric dipole $1s - 3d$ excitation was suppressed by about two orders of magnitude, when compared to the $1s - 2p$ excitation. In practice, the number of fine-structure transitions grew rapidly for open-shell atoms and ions and made then further restrictions necessary, especially if two or more open shells occur already for the ionic bound states. The uncertainty of the collision strengths for such inner-shell excitations was expected to be ~20% for electric-dipole-allowed transitions and within a factor of two for non-dipole transitions, quite similar as for the computation of the transition probabilities [31,57].
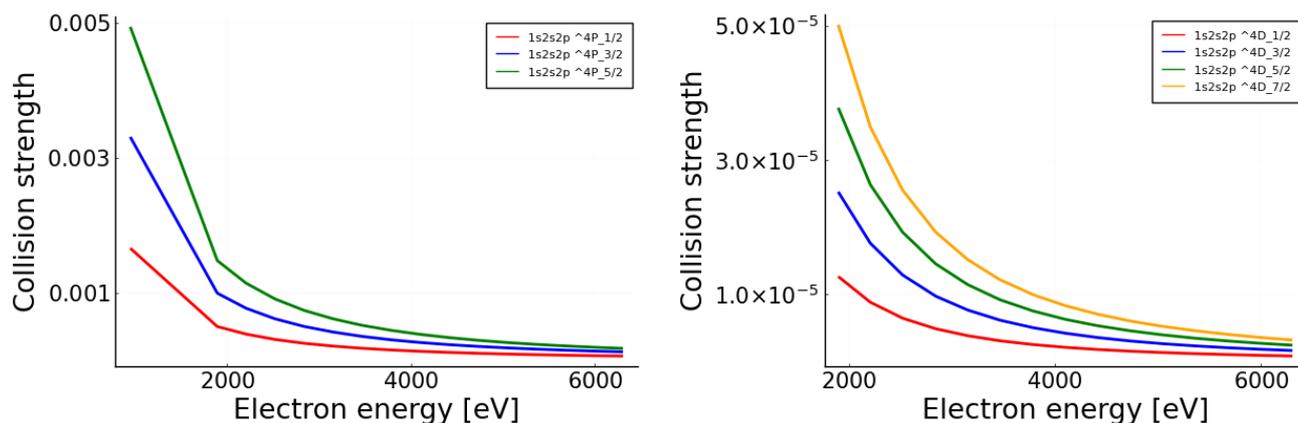
Figure 5. Collision strength $\Omega(\varepsilon_i; i \to f)$ as a function of the initial electron energy ε (eV) for different fine-structure transitions of lithium-like ions Ne^{7+}. (**Left**): Calculations for the $1s^2 2s \, ^2S_{1/2} - 1s 2s 2p \, ^4P_J$ levels with $J = 1/2$ (red line), $J = 3/2$ (blue line), and $J = 5/2$ (green line). (**Right**): The same, but for the $1s^2 2s \, ^2S_{1/2} - 1s 2s 3d \, ^4P_J$ levels with $J = 1/2, 3/2, 5/2,$ and $7/2$, respectively.

3.2. Collision Strengths for Chlorine-like Ions

Emission lines from various chlorine-like ions have been observed in a number of astrophysical sources, such as the solar corona [58], stellar chromospheres [59], or the interstellar medium [60]. The intensity ratios of these lines are typically temperature- and density-sensitive, and they can thus be utilized for the diagnostics of astrophysical plasma. If combined with EIE cross-sections, the observed line intensities can be used also to determine the elemental abundances and/or ionized equilibrium of different charge states. Chlorine-like ions are, therefore, a good test-bed to analyze and compare the EIE cross-sections and collision strengths of multiply charged ions.

Two prominent low-lying levels of chlorine-like ions refer to the (Ne) $3s^2 3p^5 \, ^2P_{3/2} - 3s \, 3p^6 \, ^2S_{1/2}$ valence shell excitation of a $3s$ subvalence electron [61]. For these excitations, the left panel of Figure 6 displays the collision strengths as a function of the initial electron energy ε for chlorine-like Ca^{3+} (red lines), Fe^{9+} (blue lines), and Mo^{25+} (green lines). The results for the $3s^2 3p^5 \, ^2P_{3/2} - 3s \, 3p^6 \, ^2S_{1/2}$ excitation (solid line) were compared with the $3s^2 3p^5 \, ^2P_{1/2} - 3s \, 3p^6 \, ^2S_{1/2}$ (dashed) line for Ca^{3+} ions. The resonant enhancement of the collision strength close to the threshold rapidly decreased, along with the strength itself, for all higher charge states. This behavior followed similar scaling rules as worked out by Kim and coworkers for neutral atoms [7]. Again, the strength of excitation from the $^2P_{1/2}$ level was about half of those for $^2P_{3/2}$ due to the statistical weight. No collision strengths were considered for electron energies close to the excitation threshold where correlations may play a more prominent role. Analog results are shown in the right panel of Figure 6, but for the $1s^2 2s^2 2p^6 3s^2 3p^5 \, ^2P_{3/2} - 1s^2 2s 2p^6 3s^2 3p^6 \, ^2S_{1/2}$ excitation of a $2s$ inner-shell electron. For these $2s - 3p$ inner-shell excitations, the collision strength was suppressed by more than two orders of magnitude. Besides core–valence correlations, these inner-shell excitations will likely be affected also by shake-up transitions of one of the valence electrons. However, the treatment of such shake-up contributions is beyond the scope of DW calculations. In EBIT, such inner-shell excitations are readily observed by its subsequent fluorescence, which have been analyzed for their angular distribution and polarization.
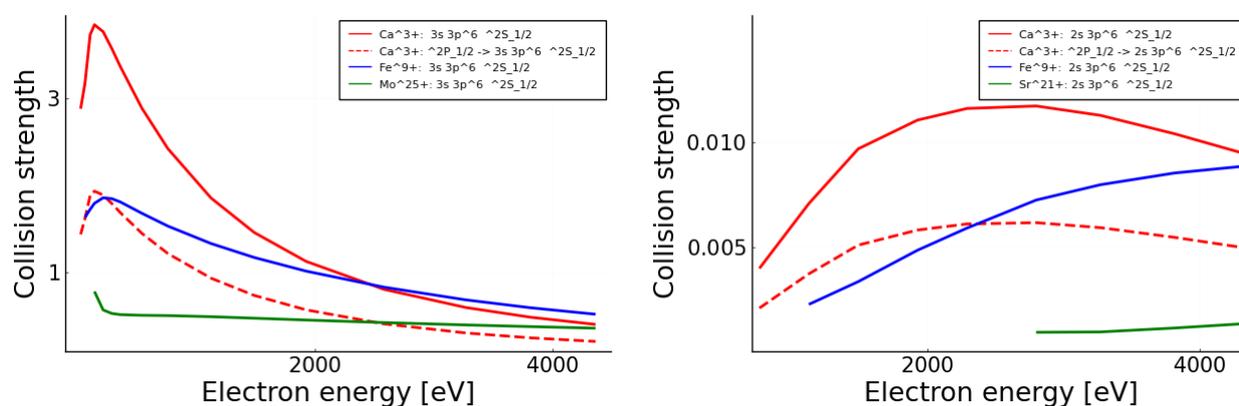
Figure 6. Collision strength $\Omega(\varepsilon; i \rightarrow f)$ as a function of the initial electron energy ε (eV) for chlorine-like Ca^{3+} (red lines), Fe^{9+} (blue lines), and Mo^{25+} (green lines). Results are shown in the (**left panel**) for the $3s^2 3p^5\,^2P_{3/2} - 3s 3p^6\,^2S_{1/2}$ excitation (solid lines) and were compared with the $3s^2 3p^5\,^2P_{31/2} - 3s 3p^6\,^2S_{1/2}$ (dashed) line for Ca^{3+} ions. The (**right panel**) shows the same, but for the $1s^2 2s^2 2p^6 3s^2 3p^5\,^2P_{3/2} - 1s^2 2s 2p^6 3s^2 3p^6\,^2S_{1/2}$ inner-shell excitation. No collision strengths were considered for electron energies close to the excitation threshold.

4. Summary and Conclusions

To analyze and provide quick access to the strength of EIE processes for multiply (and highly) charged ions of astrophysical interest, we expanded JAC, the Jena Atomic Calculator, for rapid computations of distorted wave collision strength for fine-structure-resolved, as well as configuration-averaged transitions. While we presently restricted our implementation to the direct part of the inelastic scattering amplitude, excluding the formation of dielectronic resonances, these tools can be readily applied to compute collision strengths for ions with complex shell structures. Being part of JAC, the present implementation included relativistic contributions due to both Dirac's equation and the relativistic (Breit) interaction among the electrons. It also facilitates the simple control of all input parameters, such as the selection of individual fine-structure transitions, the choice of the e–e interaction operator, or the units in compiling collision strengths and related properties as a function of the incoming energy. Several features of these tools were demonstrated for the collision strengths of low-lying excitations and inner-shell transitions.

When compared with other, explicitly correlated methods, the present expansion of the JAC toolbox supports surveys over a wide range of impact energies, levels, and/or ions. It also provides the key components to calculate effective collision strengths and EIE cross-sections for various shell structures and charge states of elements. The present expansion (may), therefore, help overcome difficulties due to the large number of notations, averaging procedures, and couplings that appear in the literature.

In the future, JAC can be enlarged to the computation of EIE plasma rate coefficients, including the dielectronic capture with subsequent autoionization. This is realized most easily by a cascade model [47] in which all relevant configurations are generated automatically, quite analogous to the computation of dielectronic recombination (DR) plasma rate coefficients. While such a cascade model treats the resonances in the cross-section *additively* to the direct excitation process, it allows incorporating—the fine structure of—all electron configurations as they are populated during the dielectronic capture of the ions. Here, emphasis will be placed mainly on those features that receive attention by the community.

Author Contributions: Methodology, S.F. and J.E.S.; software, S.F. and Y.-C.W.; writing—review and editing, S.F., L.-G.J. and J.E.S. All authors have read and agreed to the published version of the manuscript.

Institutional Review Board Statement: Not applicable.

Data Availability Statement: All data in Figures 4–6 can be reconstructed by means of the JAC toolbox, provided at the website [21].

Conflicts of Interest: The authors declare no conflict of interest.

Note

[1]   Julia comes with a full-featured interactive and command-line REPL (read-eval-print loop) that is built into the executable of the language.

References

1.   Boffard, J.B.; Lin, C.C.; DeJoseph, C.A., Jr. Application of excitation cross-sections to optical plasma diagnostics. *J. Phys. D* **2004**, *37*, R143. [CrossRef]
2.   Gupta, S.; Gangwar, R.K.; Srivastava, R. Diagnostics of Ar/N2 mixture plasma with detailed electron impact argon fine-structure excitation cross-sections. *Spectrochim. Acta B* **2018**, *149*, 213. [CrossRef]
3.   Fisher, V.; Bernshtam, V.; Golten, H.; Maron, Y. Electron-impact excitation cross-sections for allowed transitions in atoms. *Phys. Rev. A* **1996**, *53*, 2425. [CrossRef]
4.   Fontes, C.J.; Zhang, H.L.; Abdallah, J., Jr. An overview of relativistic distorted-wave cross-sections. *AIP Conf. Proc.* **2004**, *730*, 41.
5.   Kowalski, P.M.; Saumon, D. Radiative transfer in the refractive atmospheres of very cool white dwarfs. *Astrophys. J.* **2004**, *607*, 970. [CrossRef]
6.   Schreier, R.; Eviatar, A.;Vasyliūnas, V.M. A two-dimensional model of plasma transport and chemistry in the Jovian magnetosphere. *J. Geophys. Res. Planets* **1998**, *103*, 19901. [CrossRef]
7.   Kim, Y.K. Scaling of plane wave Born cross-sections for electron impact excitation of neutral atoms. *Phys. Rev. A* **2001**, *64*, 032713. [CrossRef]
8.   Elizarov, A.Y.; Tupitsyn, I.I. Calculation by plane wave Born approximation of the electron impact ionization of Ne, Ar, Kr and Xe. *Phys. Scr.* **2007**, *76*, 706. [CrossRef]
9.   Pradhan, E.K. Collision strength for [O II] and [S II]. *Mon. Not. R. Astron. Soc.* **1976**, *177*, 31. [CrossRef]
10.   Itikawa, Y. Distorted-wave methods in electron impact excitation. *Phys. Rep.* **1986**, *143*, 69. [CrossRef]
11.   Madison, D.H.; Al-Hagan, O. The distorted wave Born approach for calculating electron impact ionization of molecules. *J. Atom. Mol. Phys.* **2010**, *2010*, 367180. [CrossRef]
12.   Zhang, H.L.; Sampson, D.H.; Mohanty, A.K. Fully relativistic and quasirelativistic distorted wave methods for calculating collision strengths for highly charged ions. *Phys. Rev. A* **1989**, *40*, 616. [CrossRef] [PubMed]
13.   Zhang, H.L.; Sampson, D.H.; Clark, R.E.H. Relativistic cross-sections for excitation of highly charged ions to specific magnetic sublevels by an electron beam. *Phys. Rev. A* **1990**, *41*, 198. [CrossRef]
14.   Zhang, H.L.; Sampson, D.H.; Fontes, C.J. Relativistic distorted wave collision strengths and oscillator strengths for the 85 Li-like ions with $8 \leq Z \leq 92$. *At. Data Nucl. Data Tables* **1990**, *44*, 31. [CrossRef]
15.   Fritzsche, S. A fresh computational approach to atomic structures, processes and cascades. *Comp. Phys. Commun.* **2019**, *240*, 1. [CrossRef]
16.   Sharma, L.; Surzhykov, A.; Srivastava, R.; Fritzsche, S. Electron-impact excitation of singly charged metal ions. *Phys. Rev. A* **2011**, *83*, 062701. [CrossRef]
17.   Kim, Y.-K.; Desclaux, J.P. Relativistic effects in electron-atom collisions. *Phys. Scr.* **1987**, *36*, 796. [CrossRef]
18.   Fritzsche, S. RATIP – A toolbox for studying the properties of open-shell atoms and ions. *J. Elec. Spec. Rel. Phenom.* **2001**, *114–116*, 1155. [CrossRef]
19.   Fritzsche, S. Dielectronic recombination strengths and plasma rate coefficients of multiply charged ions. *Astron. Astrophys.* **2021**, *656*, A163. [CrossRef]
20.   Fritzsche, S. Application of symmetry-adapted atomic amplitudes. *Atoms* **2022**, *10*, 127. [CrossRef]
21.   Fritzsche S. JAC: User Guide, Compendium & Theoretical Background. Available online: https://github.com/OpenJAC/JAC.jl (accessed on 10 March 2023).
22.   Seaton, M.J. Electron excitation of forbidden lines occurring in gaseous nebulae. *Proc. R. Soc. A* **1953**, *218*, 400.
23.   Jauch, J.M.; Rohrlich, F. *The Theory of Photons and Electrons*; Springer: Berlin/Heidelberg, Germany, 2011.
24.   Sochi, T.; Storey, P.J. Methods for analyzing resonances in atomic scattering. *Eur. Phys. J. Plus* **2013**, *128*, 82. [CrossRef]
25.   Grant, I.P. *Relativistic Quantum Theory of Atoms and Molecules: Theory and Computation*; Springer: Berlin/Heidelberg, Germany, 2007.
26.   Fritzsche S. The RATIP program for relativistic calculations of atomic transition, ionization and recombination properties. *Comp. Phys. Commun.* **2012**, *183*, 1525. [CrossRef]
27.   Eliav, E.; Fritzsche, S.; Kaldor, U. Electronic structure theory of the superheavy elements. *Nucl. Phys. A* **2015**, *944*, 518. [CrossRef]
28.   Tuilkki, J. Multiple excitation at xenon 5s photoionization threshold. *Phys. Rev. Lett.* **1987**, *62*, 2817. [CrossRef]
29.   Fritzsche, S.; Fricke, B.; Sepp W.D. Reduced L_1 level-width and Coster-Kronig yields by relaxation and continuum interactions in atomic zinc. *Phys. Rev. A* **1992**, *45*, 1465. [CrossRef] [PubMed]
30.   Aggarwal, K.M.; Owada, R.; Igarashi, A. Collision strengths and effective collision strengths for allowed transitions among the $nle5$ degenerate levels of atomic hydrogen. *Atoms* **2018**, *6*, 37. [CrossRef]

31.   Fritzsche S. Large–scale accurate structure calculations for open–shell atoms. *Phys. Scr.* **2002**, *T100*, 37. [CrossRef]
32.   Fritzsche, S.; Zschornack, G.; Musiol, G.; Soff, G. Interchannel interactions in highly energetic radiationless transitions of neonlike ions. *Phys. Rev. A* **1991**, *44*, 388. [CrossRef]
33.   Fritzsche, S.; Surzhykov, A.; Stöhlker, T. Dominance of the Breit interaction in the X-ray emission of highly charged ions following dielectronic recombination. *Phys. Rev. Lett.* **2009**, *103*, 113001. [CrossRef]
34.   Gaigalas, G.; Fritzsche, S.; Grant, I.P. Calculation of angular coefficients in *jj*-coupling. *Comput. Phys. Commun.* **2001**, *139*, 263. [CrossRef]
35.   Gaigalas, G.; Fritzsche, S. Angular coefficients for symmetry-adapted configuration states in *jj*-coupling. *Comput. Phys. Commun.* **2021**, *267*, 108086. [CrossRef]
36.   Bar-Shalom, A.; Klapisch, M.; Oreg, J. Electron collision excitations in complex spectra of ionized heavy atoms. *Phys. Rev. A* **1988**, *38*, 1773. [CrossRef] [PubMed]
37.   Pindzola, M.S.; Badnell, N.R.; Henry, R.J.W.; Griffin, D.C.; Van Wyngaarden, W.L. Close-coupling calculations for the electron impact excitation of Zn^+. *Phys. Rev. A* **1991**, *44*, 5628. [CrossRef] [PubMed]
38.   Ishikawa, Y.; Vilkas, M.J. Relativistic *R*-matrix close-coupling method based on the effective many-body Hamiltonian: Benchmarks on the electron impact excitations of the Kr^{6+} ion. *Phys. Rev. A* **2008**, *77*, 052701. [CrossRef]
39.   Pindzola, M.S.; Colgan, J.; Robicheaux, F.; Griffin, D.C. Time-dependent close-coupling calculations for the electron impact ionization of carbon and neon. *Phys. Rev. A* **2000**, *62*, 042705. [CrossRef]
40.   Zatsarinny, O. A compilation of Atomic Code for Bound-State and R-Matrix Computations. Available online: https://github.com/zatsaroi (accessed on 10 April 2021).
41.   Zhang, H.L.; Pradhan, A.K. Atomic data from the Iron Project-XXVII. Electron impact excitation collision strengths and rate coefficients for Fe IV. *Astron. Astrophys. Suppl. Ser.* **1997**, *126*, 373–378. [CrossRef]
42.   Aggarwal, K.M.; Keenan, F.P.; Lawson, K.D. Electron impact excitation of N IV: Calculations with the DARC code and a comparison with ICFT results. *Mon. Not. R. Astron. Soc.* **2016**, *461*, 3997. [CrossRef]
43.   Tayal, S.S. Oscillator strengths and effective collision strengths for electron excitation of Mg VI. *Astron. Astrophys.* **2012**, *548* A27. [CrossRef]
44.   Fritzsche, S. Level structure and properties of open *f*-shell elements. *Atoms* **2022**, *10*, 7. [CrossRef]
45.   Available online: https://docs.julialang.org/ (accessed on 10 February 2021).
46.   Fritzsche, S.; Maiorova, A.V.; Wu, Z.W. Radiative recombination plasma rate coefficients for multiply charged ions. *Atoms* **2023**, *11*, 50. [CrossRef]
47.   Fritzsche, S.; Palmeri, P.; Schippers, S. Atomic cascade computations. *Symmetry* **2021**, *13*, 520. [CrossRef]
48.   Schippers, S.; Martins, M.; Beerwerth, R.; Bari, S.; Holste, K.; Schubert, K.; Jens, V.; Savin Daniel, W.; Fritzsche, S.; Müller, A. Near L-edge single and multiple photoionization of singly charged iron ions. *Astrophys. J.* **2017**, *849*, 5. [CrossRef]
49.   Beerwerth, R.; Buhr, T.; Perry-Sassmannshausen A.; Stock, S.O.; Bari, S.; Holste, K.; Kilcoyne, A.L.D.; Reinwardt, S.; Ricz, S.; Savin, D.W.; et al. Near L-edge single and multiple photoionization of triply charged iron ions. *Astrophys. J.* **2019**, *887*, 189. [CrossRef]
50.   Schippers, S.; Beerwerth, R.; Bari, S.; Buhr, T.; Holste, K.; Kilcoyne, A.L.D.; Perry-Sassmannshausen, A.; Phaneuf, R.A.; Reinwardt, S.; Savin, D.W.; et al. Near L-edge single and multiple photoionization of doubly charged iron ions. *Astrophys. J.* **2021**, *908*, 52. [CrossRef]
51.   Sahoo, A.K.; Sharma, L. Electron impact excitation of extreme ultra-violet transitions in Xe^{7+}–Xe^{10+} ions. *Atoms* **2021**, *9*, 76. [CrossRef]
52.   Zhang, H.L.; Sampson, D.H. Relativistic distorted wave collision strengths and oscillator strengths for all possible $n = 2 - n = 3$ transitions in B-like ions. *At. Data Nucl. Data Tables* **1994**, *58*, 255. [CrossRef]
53.   Bhatia, A.K. Superstructure and distorted wave codes and their application. *Atoms* **2022**, *10*, 47. [CrossRef]
54.   Malker, P.; Sharma, L. Electron impact excitation of Ge-like Te^{20+} - Cd^{16+} ions. *Atoms* **2022**, *10*, 17. [CrossRef]
55.   Storey, P.J.; Sochi, A. Collision strengths and transition probabilities for Co III forbidden lines. *Mon. Not. R. Astron. Soc.* **2016**, *459*, 2558. [CrossRef]
56.   Inal, M.K.; Dubau, J. Theory of excitation of He-like and Li-like atomic sublevels by directive electrons: Application to X-ray line polarisation. *J. Phys. B* **1987**, *20*, 4221. [CrossRef]
57.   Kohstall, C.; Fritzsche, S.; Fricke, B.; Sepp, W.-D. Calculated level energies, transition probabilities and lifetimes of silicon–like ions. *At. Data Nucl. Data Tables* **1998**, *70*, 63. [CrossRef]
58.   Jupen, C.; Bengtsson, P.; Engström, L.; Livingston, A.E. The $2s^2 2p^3 3s, 3p$ and $3d$ configurations in nine times ionized chlorine, Cl X. *Phys. Scr.* **2001**, *64*, 329. [CrossRef]
59.   Judge, P.; Bryans, P.; Casini, R.; Kleint, L.; Lacatus, D.; Paraschiv, A.; Schmit, D. Optimal spectral lines for measuring chromospheric magnetic fields. *Astrophys. J.* **2022**, *941*, 159. [CrossRef]
60.   Moomey, D.; Federman, S.R.; Sheffer, Y. Revisiting the chlorine abundance in diffuse interstellar clouds from measurements with the copernicus satellite. *Astrophys. J.* **2012**, *744*, 174. [CrossRef]
61.   Dong, C.Z.; Fritzsche, S.; Fricke, B.; Sepp, W.-D. Branching ratios and lifetimes of the low–lying levels of Fe X. *Mon. Not. R. Astron. Soc.* **1999**, *307*, 809. [CrossRef]